Available online at www.sciencedirect.com

ScienceDirect

Ceramics International 41 (2015) 8735–8741

CERAMICS INTERNATIONAL

www.elsevier.com/locate/ceramint

Fabrication and characterization of copper doped TiO_2 nanotube arrays by in situ electrochemical method as efficient visible-light photocatalyst

Mohamad Mohsen Momeni*, Yousef Ghayeb, Zohre Ghonchegi

Department of Chemistry, Isfahan University of Technology, Isfahan 84156-83111, Iran

Received 1 November 2014; received in revised form 27 February 2015; accepted 18 March 2015
Available online 27 March 2015

Abstract

Highly ordered copper doped TiO_2 nanotube arrays ($CuTiO_2NTs$) thin-film were prepared in an aqueous solution containing NH_4F and different concentrations of copper nitrate via the electrochemical oxidation of titanium substrates. The resulting nanotubes were characterized by FE-SEM, XRD, XPS and EDX. The $CuTiO_2NTs$ showed a tube diameter of 40–90 nm and wall thickness of 20–30 nm. Diffuse reflectance spectra showed a shift toward longer wavelengths relative to pure TiO_2 nanotubes (TiO_2NTs). The visible light photo-catalytic activity of the $CuTiO_2NTs$ electrodes was evaluated by the removal of methylene blue (MB) dye and the production of hydrogen. The results showed that $CuTiO_2NTs$ samples exhibited better photo-catalytic activity than the TiO_2NTs. This work demonstrated a feasible and simple anodization method to fabricate an effective, reproducible, and inexpensive visible-light-driven photo-catalyst for hydrogen evolution and environmental applications.

Keywords: TiO_2 nanotubes; Photo-catalytic; Hydrogen evolution; Copper doping; Anodization

1. Introduction

Among the semiconductor oxides, TiO_2 has been widely used as the most suitable material for environmental photo-catalytic applications because of its biological and chemical inertness, cost effectiveness, and the strong oxidizing power of its photo-generated holes [1–6]. Generally, TiO_2 with a large specific surface area can improve the photo-catalytic performance. Therefore, many efforts have been made to obtain nanostructured TiO_2-based materials with a large specific surface area [7–9]. Nanostructured titanium dioxide has been attracting attention from both fundamental and applied perspectives, driven by its unique photo-activity in a broad range of applications, extending from photo-catalysis of hazardous chemicals, self-cleaning surfaces, to solar energy conversion, gas sensors, and hydrogen storage [10–16]. One-dimensional TiO_2 nanostructures, particularly TiO_2 nanotubes, have received great attention because of their superior photo-catalytic and photo-electronic performance over TiO_2 nanoparticles. TiO_2 nanotubes have been synthesized via various approaches, including using a template of nanoporous alumina, sol–gel processes, seeded growth method, hydrothermal techniques and the anodizing of titanium plates [17–21]. Among these, anodizing of titanium is a relatively simple process for the fabrication of aligned TiO_2 nanotubes.

TiO_2 acts photo-catalytically by absorbing the ultraviolet light with a wavelength no longer than 387 nm to generate electron–hole pairs. These separated electrons (e^-) and holes (h^+) are then available to drive reduction and oxidation reactions, respectively. However, the fast electron–hole pair recombination decreases its catalytic efficiency [22]. So the key issue to improve the efficiency of the photo-catalytic process is to ensure that more photo-generated e^- and h^+ can move to the surface of the semiconductor particles before they recombine in bulk. Besides this the need of UV light for its excitation restricts the use of easily available sunlight and cheaper visible light [23]. To improve the photo-catalytic efficiency and extending the spectral response of TiO_2 nanotube to the visible spectrum, many attempts have been made such as doping metal ions such as Pt, Pd, Au and Ag.

*Corresponding author. Tel.: +98 3113912237; fax: +98 3113912350.
E-mail address: mm.momeni@cc.iut.ac.ir (M.M. Momeni).

http://dx.doi.org/10.1016/j.ceramint.2015.03.094
0272-8842/

Table 1
The experimental parameters for the prepared samples.

Samples	Anodizing solution	Condition
TiO_2NTs	0.135 M NH_4F	20 V, 60 min, 25 °C
CuTiO_2NTs-1	0.135 M NH_4F+0.041 M $Cu(NO_3)_2 \cdot 3H_2O$	20 V, 60 min, 25 °C
CuTiO_2NTs-2	0.135 M NH_4F+0.124 M $Cu(NO_3)_2 \cdot 3H_2O$	20 V, 60 min, 25 °C

The doped metal ion enhances the photo-catalytic activity by reducing electron–hole pair recombination and/or reducing the band gap. Some has successfully improved the activity of TiO_2 by doping metal ions like Au and Pt but they are very expensive and rare elements [24–29]. In this context, one potential metal dopant for TiO_2 surfaces is copper, a metal of relative abundance and low cost. Till now, very less research has been done to observe the quantity effect of copper in Cu–TiO_2 nanotubular composite on photo-catalytic activities of Cu-doped TiO_2. In the present study, we report a simple approach to fabricate copper-doped TiO_2NTs by a single-step anodization of titanium substrate in an aqueous bath containing ammonium fluoride and copper nitrate. The morphology and structure were characterized by scanning electron microscopy (SEM), energy dispersive X-ray spectroscopy (EDS), X-ray photoelectron spectrometer (XPS) and X-ray diffraction (XRD). Optical properties were investigated by UV–vis diffuse reflectance spectra. The effect of the copper doping on the visible light photo-catalytic activity of CuTiO_2NTs samples was evaluated through the degradation of methylene blue (MB) and hydrogen generation.

2. Experimental

2.1. Chemicals and solutions

Ammonium fluoride (NH_4F), methylene blue, copper (II) nitrate ($Cu(NO_3)_2 \cdot 3H_2O$), HF, H_2SO_4 and HNO_3 were of analytical grade. All solutions were prepared with distilled water.

2.2. Fabrication of Cu-doped TiO_2 nanotube electrode

The titanium foils (99.99% purity, 1-mm thick, 1 cm × 4 cm) used in anodization experiments were first mechanically polished with different emery type abrasive papers (with the following grades: 60, 80, 600, 1200, and 2500), rinsed in a bath of distilled water, and then chemically etched by immersing in a mixture of HF and HNO_3 acids for 30 s. The ratio of components HF/HNO_3/H_2O in the mixture was 1:4:5 in volume. The last step of pretreatment was rinsing with distilled water. The anodization was conducted in a two-electrode electrochemical system with a platinum foil as the cathode at a constant potential with a direct current power supply (ADAK, PS405). The electrolyte was prepared by the dissolution of 0.135 M NH_4F and different concentrations of copper nitrate. Anodization was carried out in mentioned solutions under a constant voltage of 20 V for 60 min at room temperature. After anodization, the as-formed samples were sintered at 400 °C for 2 h (2 °C/min) to obtain copper-doped TiO_2 nanotubes denoted as CuTiO_2NTs. For comparison, undoped TiO_2 nanotubes denoted as pure TiO_2NTs was prepared in the same way except that $Cu(NO_3)_2 \cdot 3H_2O$ was absent in the process. The concentration of copper nitrate in anodizing solution was 0, 0.041 and 0.124 M/L, respectively. Table 1 summarizes the experimental conditions for 3 different samples.

2.3. Characterization

The surface morphology of all samples were characterized by field emission scanning electron microscopy (FE-SEM, Hitachi S-4160, Japan), and the elemental composition was estimated by energy dispersive X-ray spectroscopy (EDX). The crystalline phases were identified by XRD (Philips X'Pert). Diffraction patterns were recorded in the 2θ range from 20 to 80° at room temperature. UV–visible absorption spectra of the samples were recorded on a photospectrometer (JASCO V-570).

2.4. Photo-catalytic activity and hydrogen generation measurements

Photo-catalytic activities of all the samples were evaluated by degradation of the aqueous methylene blue (MB) dye under visible light irradiation. The photo-catalytic reaction was carried out in a single-compartment cylindrical quartz reactor. A 200 W xenon lamp was used as a light source with a 420 nm cutoff filter to provide visible light. A fan was used to cool down the reactor tube. The experiments were performed at room temperature. The initial concentration of methylene blue (MB) was 2 mg/L. The volume of the solution was 50 mL. Prior to illumination, the photo-catalyst sample was immersed in quartz reactor containing methylene blue and magnetically stirred for 2 h in the dark to ensure the establishment of an adsorption–desorption equilibrium between the photo-catalyst and methylene blue. Then the solution was exposed to visible light irradiation under magnetic stirring for 2 h. At each 10 min intervals, 5 ml solution was sampled and the absorbance of methylene blue (MB) at 660 nm was measured by a UV–vis spectrophotometer.

The photo-catalytic hydrogen production was evaluated in 50 mL aqueous solution of 1 M NaOH. Different electrodes were illuminated with a 200 W xenon lamp that its luminous intensity was 100 W/cm^2. Hydrogen evolution was measured for 120 min and H_2 gas was collected using the water displacement technique. H_2 gas is produced at the counter-electrode in the photo-electrochemical (PEC) cell. Fig. 1 shows a schematic diagram of the experimental set-up for PEC water

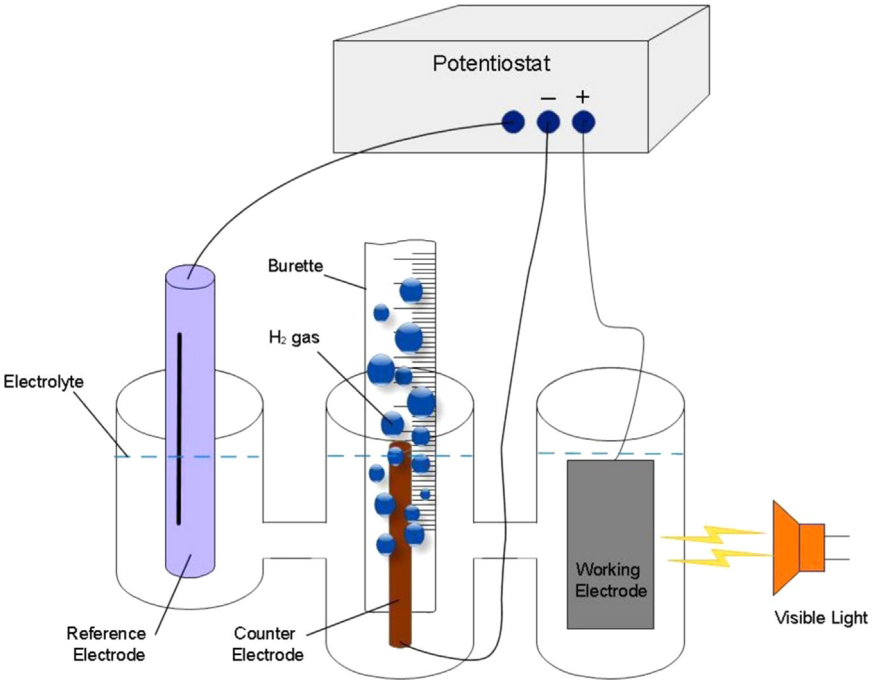

Fig. 1. Schematic diagram of the experimental set-up for photocatalytic water splitting.

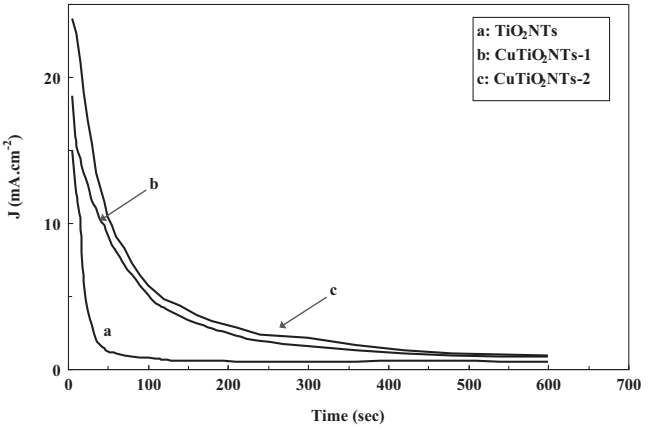

Fig. 2. Current transient curves recorded during anodizing of titanium at different concentrations of copper nitrate in electrolyte (0.135 M NH_4F solution).

splitting. A Pt coil spot-welded to a stainless steel rod served as the cathode. The cathode was inserted into a buret where the hydrogen was collected via electrolyte displacement. The volume of hydrogen was measured by directly reading the variation of the electrolyte level in the buret for various times.

3. Results and discussion

Fig. 2 shows the current transient during anodization of titanium foils, which anodized in an electrolyte of 0.135 M NH_4F+different concentrations of copper nitrate. The sharp drop of the current behavior in initial time is due to the formation of initial oxide layer and then the current reached a steady state value. The anodized current was increased with the increase in copper nitrate.

The FE-SEM of the as-prepared samples was illustrated in Fig. 3. It can be seen that the structure of as-prepared $CuTiO_2NTs$ consists of a layer of highly ordered tubes with a diameter in the range of 40–90 nm and wall thickness of 20–30 nm. The surface of them was open. The morphology of the $CuTiO_2NTs$ composites is similar to TiO_2NTs (not shown) indicating that the Cu-doping process does not influence the morphologies of the TiO_2 samples.

Fig. 4 shows the X-ray diffraction pattern of the pure TiO_2NTs and $CuTiO_2NTs$ composites film annealed at 400 °C. It confirms the presence of anatase phase of TiO_2 in the samples, and the Ti peaks were due to the Ti substrate. However, the diffraction pattern of CuO is not seen in the XRD of the doped material. This is likely due to a low composition of copper. Xu et al. reported the instances where diffraction peaks of copper species disappeared when copper component was highly dispersed in TiO_2 [30]. Therefore, it is believed that the copper components in $CuTiO_2NTs$ were highly dispersed in the samples, with small dimensions below XRD detection limit. EDS was employed to detect elemental compositions of $CuTiO_2NTs$ photo-catalysts and result is shown in Fig. 4. In EDS spectrum of $CuTiO_2NTs$, peaks of Ti, Cu, O and Au were clearly observed, where Au were attributed to the gold coating required by tests. This analysis confirms the formation of the $CuTiO_2NTs$ composites film.

The nature of the species actively present on the surface is important for establishing the properties of the catalyst. For this purpose, an XPS analysis was performed to determine the chemical state of the elements on the surface of $CuTiO_2NTs$ sample. X-ray photoelectron spectroscopy (XPS) is a quantitative spectroscopic method that determined the elemental composition, empirical-formula, chemical state, binding energy, and electronic-state of the

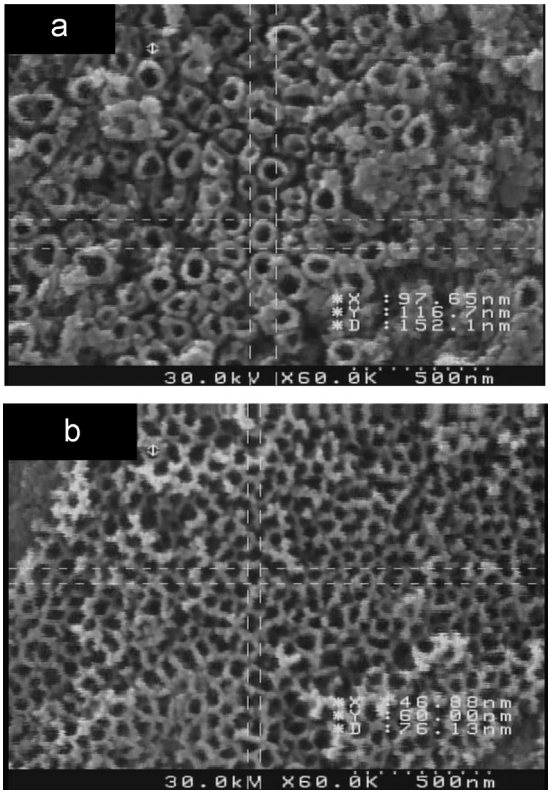

Fig. 3. SEM top-view images of the samples formed by anodic oxidation in a 0.135 M NH_4F solution containing different concentrations of copper nitrate; (a) 1 g/l (sample $CuTiO_2NTs$-1) and (b) 3 g/l (sample $CuTiO_2NTs$-2).

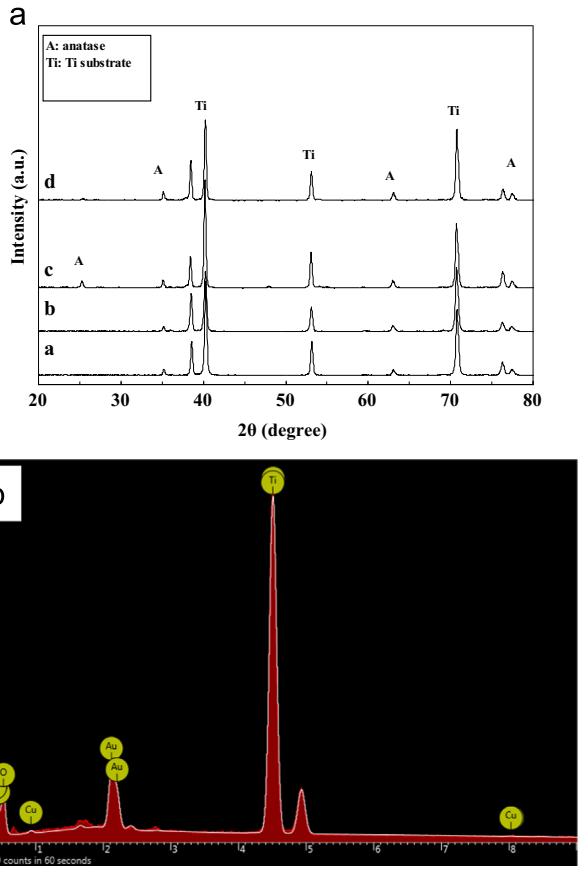

Fig. 4. (A) XRD patterns of photocatalysts [(a) as-prepared TiO_2NTs; (b) as-prepared $CuTiO_2NTs$-2; (c) TiO_2NTs annealed at 400 °C; (d): $CuTiO_2NTs$-2 annealed at 400 °C]. (B) EDX spectrum of the $CuTiO_2NTs$ sample.

elements that present within a material [31]. The elemental composition of the copper doped TiO_2 nanotube arrays ($CuTiO_2NTs$) and chemical states of CuO and TiO_2 was characterized using XPS (Fig. 5). It is clear that the surface of the TiO_2 nanotube arrays is composed of Ti, O, Cu, and C elements. No other metal ions other than Cu and Ti can be detected on the surface, which implies that the sample is not induced by other foreign impurities. In Fig. 5, the spin orbit peaks of the Cu 2p (3/2) and Cu 2p(1/2) binding energy for $CuTiO_2NTs$ sample appeared at around 939.2 eV and 959.1 eV respectively and assigned to the compound of CuO, which is in good agreement with the reference data for CuO [32]. The spin orbit peaks of the Ti 2p(3/2) binding energy for codoped sample appeared around at 459.1 eV, which is in good agreement with the reference data for TiO_2 [33]. Ti 2p(3/2) peak exists at 459.1 eV in this sample, which is 0.7 eV higher than that in pure TiO_2. This is because the Fermi levels of CuO are lower than those of TiO_2, so that the electrons of TiO_2 may transfer to CuO dispersed on the surface of TiO_2, which results in change in the outer electron cloud density of Ti. Hence, the Ti 2p binding energy increased [34]. This fact suggests that there is an intense interaction between TiO_2 and Cu species. The O 1s spectrum shows two peaks; a peak at binding energy of 530.6 eV and other at 533.7 eV. The peak at 530.6 eV is assigned to lattice oxygen presence in the $CuTiO_2NTs$ that attributed to the O in TiO_2 and CuO; whereas the peaks at higher binding energy of 533.7 eV was indicative of surface contamination by hydroxides, from the atmosphere [34–36].

The optical properties such as reflectance spectra and optical band gap energy of TiO_2NTs and $CuTiO_2NTs$ composites film were studied. Fig. 6 shows the optical band gap energy of TiO_2NTs and $CuTiO_2NTs$ composites film annealed at 400 °C, respectively. The reflectance data, reported as $F(R)$ values, have been obtained by application of the Kubelka–Munk algorithm. The band gaps of the samples have been deduced from the Tauc plot. Fig. 6 is the plot of $[F(R)h\upsilon]^{1/2}$ versus photon energy. The extrapolation of $[F(R)h\upsilon]^{1/2}$ to the abscissa at zero $F(R)$ provides the band gap energy as ~3.20 eV for TiO_2NTs and the band gap energy ~2.65 eV for $CuTiO_2NTs$ composite. These results clearly indicate that Cu was incorporated in TiO_2 lattice to extend the absorption to a long wavelength range.

Photo-catalytic activity of different photo-catalysts was followed through degradation of methylene blue (MB) as a function of irradiation time with visible light (Fig. 7). The data are plotted according to the classic pseudo-first rate approach $\ln(C_t/C_0)=kt$, where k is the rate constant and t is time. From the linear shape of the data the k values can be extracted [37]. From the obtained k values it can be seen that both $CuTiO_2NTs$ possess higher decomposition rate than pure TiO_2 nanotubes.

The stability of a photo-catalyst was also important to its practical application for it can be regenerated and reused. We

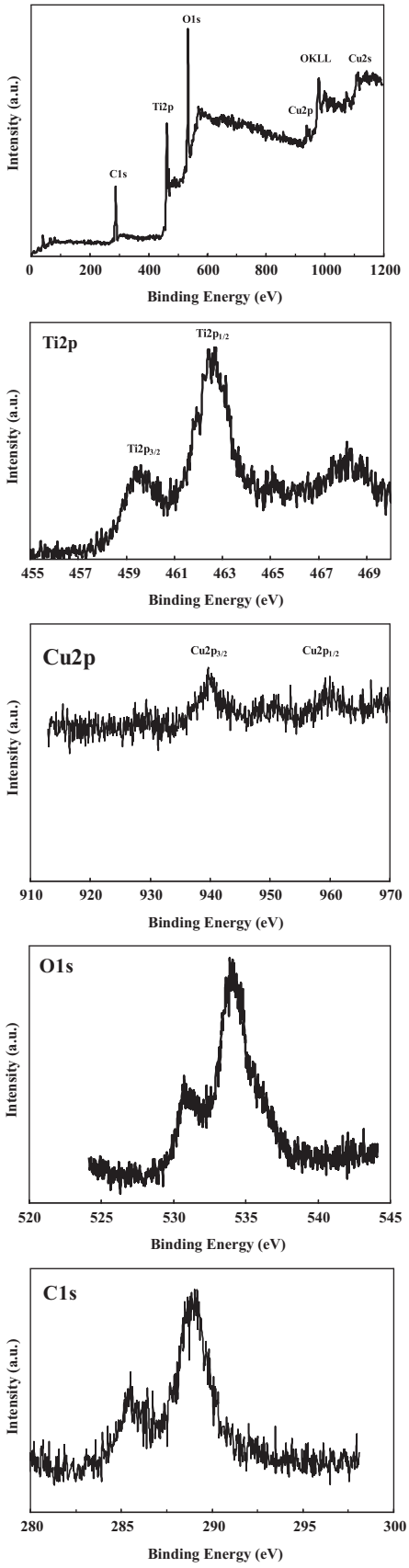

Fig. 5. XPS of $CuTiO_2$NTs sample. Ti 2p, Cu 2p, O 1s and C 1s XPS spectra of this sample.

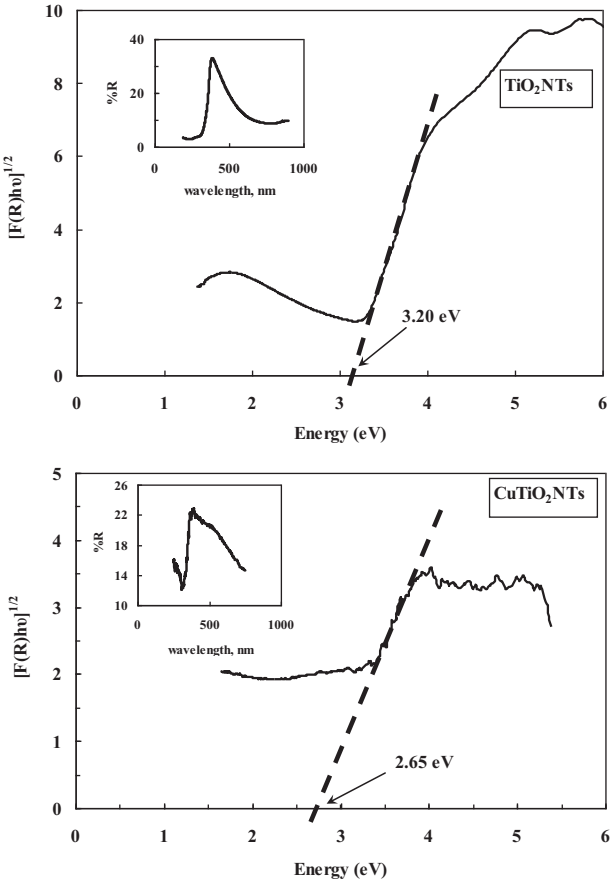

Fig. 6. Tauc plot of the pure TiO_2 nanotubes (TiO_2NTs) and $CuTiO_2$NTs-2 composites. Insets: reflectance spectra of the related samples.

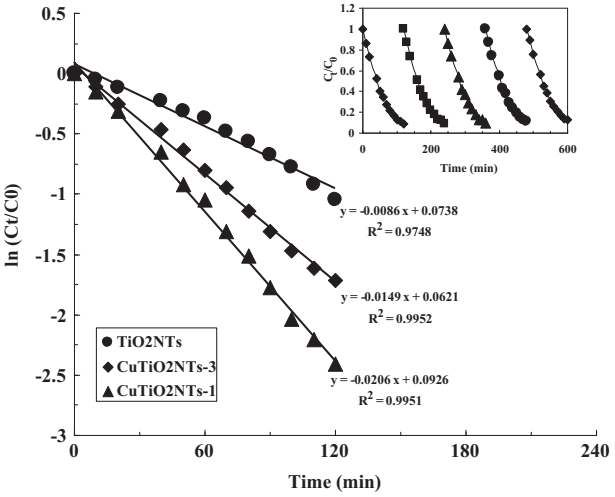

Fig. 7. The photo-catalytic degradation of MB over the different samples as ln (C_t/C_0) vs. irradiation time plot. Inset: photo-catalyst stability test of $CuTiO_2$NTs-1.

investigated the cyclic stability of $CuTiO_2$NTs-1 photocatalyst by monitoring the catalytic activity during successive cycles of use. As shown in Fig. 7 (inset), after a five-cycle experiment, the catalyst exhibited similar catalytic performance without

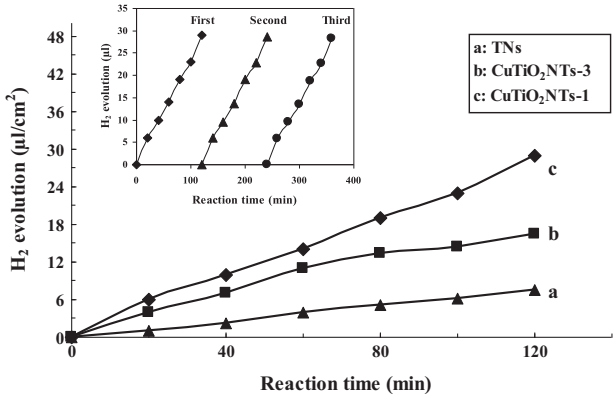

Fig. 8. Photo-catalytic H_2 production of different samples over irradiation time. Inset: the reusability of $CuTiO_2NTs$-1.

significant deactivation, revealing its high stability after multiple reuses.

In order to investigate beneficial effects of copper doping for photo-catalytic hydrogen production under visible light, we used alkaline solution. Various samples were investigated using open circuit conditions. Control experiments indicated that no appreciable hydrogen production was detected in the absence of either visible light irradiation or photo-catalyst, suggesting that hydrogen was produced by photo-catalytic reactions on photo-catalyst. Fig. 8 shows hydrogen production for different samples. It shows that H_2 production on all samples shows linear H_2 production over time. The total amount of H_2 evolved on the sample $CuTiO_2NTs$-1 was 29 $\mu L/cm^2$ 1after 120 min, which is approximately 1.76 times higher than that on the sample $CuTiO_2NTs$-1 (16.5 $\mu L/cm^2$) and 3.81 times higher than that on the TiO_2NTs (7.6 $\mu L/cm^2$). The recyclability of $CuTiO_2NTs$-1 photo-catalyst was tested during three runs of photo-catalytic reaction under visible light irradiation, as shown in Fig. 8 (inset). The amount of hydrogen evolution linearly increases as a function of the duration time and no obvious degradation occurs after three runs. These results indicate that $CuTiO_2NTs$ samples are a relatively stable photo-catalyst and can keep the activity for a period of time.

4. Conclusion

In summary, copper doped TiO_2 nanotube arrays ($CuTiO_2NTs$) fabricated via a facile and novel anodization process in a single-step process using copper (II) nitrate as the Cu source. The resulting nanotubes showed a tube diameter of 40–90 nm and wall thickness of 20–30 nm. Diffuse reflectance spectra show an improvement in the visible absorption relative to bare TiO2 nanotubes. $CuTiO_2NTs$ composites have excellent photo-catalytic performance. Copper doping was found to improve the photo-catalytic performance of TiO_2NTs. These $CuTiO_2NTs$ nanotubular composite are interesting candidates to drive photochemical reactions, such as water reduction (H_2 production) and oxidation of pollutants. The novel anodization process developed in this study is simple and effective method and can be easily scaled up, thereby pioneering the fabrication of high performance metal-doped TiO_2NTs photo-catalysts with promising environmental applications.

References

[1] R. Lopez, R. Gomez, M.E. Llanos, Photophysical and photocatalytic properties of nanosized copper-doped titania sol–gel catalysts, Catal. Today 148 (2009) 103–108.
[2] G. Wu, J. Wang, D.F. Thomas, A. Chen, F-doped flower-like TiO_2 nanostructures with high photocatalytic activity, Langmuir 24 (2008) 3503–3509.
[3] G. Wu, A. Chen, Direct growth of F-doped TiO_2 particulate thin films with high photocatalytic activity for environmental applications, J. Photochem. Photobiol. A: Chem. 195 (2008) 47–53.
[4] A.G. Munoz, Semiconducting properties of self-organized TiO_2 nanotubes, Electrochim. Acta 52 (2007) 4167–4176.
[5] Y.H. Zhang, H.L. Xu, Y.X. Xu, H.X. Zhang, Y.G. Wang, The effect of lanthanide on the degradation of RB in nanocrystalline Ln/TiO_2 aqueous solution, J. Photochem. Photobiol. A: Chem. 170 (2005) 279–285.
[6] Y.Y. Hou, J.M. Hu, L. Liu, J.Q. Zhang, C.N. Cao, Effect of calcination temperature on electrocatalytic activities of Ti/IrO_2 electrodes in methanol aqueous solutions, Electrochim. Acta 51 (2006) 6258–6267.
[7] M. Salari, S.M. Mousavikhoie, P. Marashi, M. Rezaee, Synthesis of TiO_2 nanoparticles via a novel mechanochemical method, J. Alloy. Compd. 469 (2009) 386–390.
[8] Q.J. Li, B.B. Liu, Y.G. Li, R. Liu, X.L. Li, D.M. Li, S.D. Yu, D.D. Liu, P. Wang, B. Li, B. Zou, T. Cui, G.T. Zou, Ethylene glycol-mediated synthesis of nanoporous anatase TiO_2 rods and rutile TiO_2 self-assembly chrysanthemums, J. Alloy. Compd. 471 (2009) 477–480.
[9] H. Yanga, C. Pan, Diameter-controlled growth of TiO_2 nanotube arrays by anodization and its photoelectric property, J. Alloy. Compd. 492 (2010) L33–L35.
[10] R. Armon, G. Weltch-Cohen, P. Bettane, Disinfection of Bacillus spores in drinking water by TiO_2 photocatalysis as a model for *Bacillus anthracis*, Water Sci. Technol. 4 (2004) 7–14.
[11] Y. Ohko, T. Tatsuma, T. Fujii, K. Naoi, C. Niwa, Y. Kubota, A. Fujishima, TiO_2 film loaded with silver nanoparticles: control of multicolor photochoromic behavior, Nat. Mater. 2 (2003) 29–31.
[12] A. Bozzi, T. Yuranova, J. Kiwi, Self-cleaning of wool-polyamide and polyester textiles by TiO_2-rutile modification under daylight irradiaton at ambient temperature, J. Photochem. Photobiol.: A 172 (2005) 27–34.
[13] G.K. Mor, O.K. Varghese, M. Paulose, K. Shankar, C.A. Grimes, A review on higly ordered, vertically oriented TiO_2 nanotube arrays: fabrication, material properties, and solar energy application, Sol. Energy Mater. Sol. Cells 90 (2006) 2011–2075.
[14] C. Garzella, E. Comini, E. Tempesti, C. Frigeri, G. Sberveglieri, TiO_2 thin films by a novel sol–gel processing for gas sensor applications, Sens. Actuators: B. 68 (2000) 189–196.
[15] D.V. Bavykin, A.A. Lapkin, P.K. Plucinski, J.M. Friedrich, F.C. Walsh, Reversible storage of molecular hydrogen by sorption into multilayered TiO_2 nanotubes, J. Phys. Chem. B 109 (2005) 19422–19427.
[16] P. Pillai, K.S. Raja, M. Misra, Electrochemical storage of hydrogen in nanotubular TiO_2 arrays, J. Power Sources 161 (2006) 524–530.
[17] H. Imai, Y. Takei, K. Shimizu, M. Matsuda, H. Hirashima, Direct preparation of anatase TiO_2 nanotubes in porous alumina membranes, J. Mater. Chem. 9 (1999) 2971–2972.
[18] J.H. Jung, H. Kobayashi, K.J.C. van Bommel, S. Shinkai, T. Shimizu, Creation of novel helical ribbon and double-layered nanotube TiO_2 structures using an organogel template, Chem. Mater. 14 (2002) 1445–1447.
[19] Z.R.R. Tian, J.A. Voigt, J. Liu, B. McKenzie, H.F. Xu, Large oriented arrays and continuous films of TiO_2-based nanotubes, J. Am. Chem. Soc. 125 (2003) 12384–12385.
[20] X. Peng, A. Chen, Aligned TiO_2 nanorod arrays synthesized by oxidizing titanium with acetone, J. Mater. Chem. 14 (2004) 2542–2548.

[21] H. Li, J. Wang, K. Huang, G. Sun, M. Zhou, In-situ preparation of multi-layer TiO_2 nanotube array thin films by anodic oxidation method, Mater. Lett. 65 (2011) 1188–1190.
[22] J. Tang, J.R. Durrant, D.R. Klug, Mechanism of photocatalytic water splitting in TiO_2. Reaction of water with photoholes, importance of charge carrier dynamics, and evidence for four-hole chemistry, J. Am. Chem. Soc. 130 (2008) 13885–13891.
[23] J. Zhao, T. Wu, K. Wu, K. Oikawa, H. Hidaka, Photoassisted degradation of dye pollutants. 3. Degradation of the cationic dye rhodamine B in aqueous anionic surfactant/TiO_2 dispersions under visible light irradiation: evidence for the need of substrate adsorption on TiO_2 particles, Environ. Sci. Technol. 32 (1998) 2394–2400.
[24] S. Sakthivel, M.V. Shankar, M. Palanichamy, B. Arabindoo, D. W. Bahnemann, V. Murugesan, Enhancement of photocatalytic activity by metal deposition: characterisation and photonic efficiency of Pt, Au and Pd deposited on TiO_2 catalyst, Water Res. 38 (2004) 3001–3008.
[25] B. Xin, L. Jing, Z. Ren, B. Wang, H. Fu, Effects of simultaneously doped and deposited Ag on the photocatalytic activity and surface states of TiO_2, J. Phys. Chem. B 109 (2005) 2805–2809.
[26] L. Zang, C. Lange, I. Abraham, S. Storck, W.F. Maier, H. Kisch, Amorphous microporous titania modified with platinum(IV) chloride–a new type of hybrid photocatalyst for visible light detoxification, J. Phys. Chem. B 102 (1998) 10765–10771.
[27] V. Subramanian, E. Wolf, P.V. Kamat, Semiconductor–metal composite nanostructures. To what extent metal nanoparticles (Au, Pt, Ir) improve the photocatalytic activity of TiO_2 films, J. Phys. Chem. B 105 (2001) 11439–11446.
[28] R. Chand, E. Obuchi, K. Katoh, H.N. Luitel, K. Nakano, Enhanced photocatalytic activity of TiO_2/SiO_2 by the influence of Cu-doping under reducing calcination atmosphere, Catal. Commun. 13 (2011) 49–53.
[29] H. Li, J. Wang, M. Liu, H. Wang, P. Su, J. Wu, J. Li, A nanoporous oxide interlayer makes a better Pt catalyst on a metallic substrate: nanoflowers on a nanotube bed, Nano Res. 7 (2014) 1007–1017.
[30] B. Xu, L. Dong, Y. Chen, Influence of CuO loading on dispersion and reduction behavior of CuO/TiO_2 (anatase) system, J. Chem. Soc. Faraday Trans. 94 (1998) 1905–1909.
[31] M.M. Rahman, S.B. Khan, H.M. Marwani, A.M. Asiri, K.A. Alamry, Selective Iron(III) ion uptake using CuO–TiO_2 nanostructure by inductively coupled plasma-optical emission spectrometry, Chem. Cent. J. 6 (2012) 158–168.
[32] C.C. Chusuei, M.A. Brookshier, D.W. Goodman, Correlation of relative x-ray photoelectron spectroscopy shake-up intensity with CuO particle size, Langmuir 15 (1999) 2806–2808.
[33] R.G. Palgrave, D.J. Payne, R.G. Egdell, Nitrogen diffusion in doped TiO_2 (110) single crystals: a combined XPS and SIMS study, J. Mater. Chem. 19 (2009) 8418–8425.
[34] H. Liu, Y. Wang, G. Liu, Y. Ren, N. Zhang, G. Wang, T. Li, An energy-efficient electrochemical method for CuO–TiO_2 nanotube array preparation with visible-light responses, Acta Metall. Sin. 27 (1) (2014) 149–155.
[35] Y. Su, S. Chen, X. Quan, H. Zhao, Y. Zhang, A silicon-doped TiO_2 nanotube arrays electrode with enhanced photoelectrocatalytic activity, Appl. Surf. Sci. 255 (2008) 2167–2172.
[36] S. Xu, A.J. Du, J. Liu, J. Ng, D.D. Sun, Highly efficient CuO incorporated TiO_2 nanotube photocatalyst for hydrogen production from water, Int. J. Hydrog. Energy 36 (2011) 6538–6545.
[37] M.M. Momeni, Y. Ghayeb, M. Davarzadeh, Electrochemical construction of different titania–tungsten trioxide nanotubular composite and their photocatalytic activity for pollutant degradation: a recyclable photocatalysts, J. Mater. Sci: Mater. Electron. 26 (2015) 1560–1567.